High Time Resolution Q-Band EPR Study of Sequential Electron Transfer in a Triad Oriented in a Liquid Crystal†

Ulrich Heinen,‡ Thomas Berthold,‡ Gerd Kothe,*,‡ Eli Stavitski,§ Tamar Galili,§ Haim Levanon,*,§ Gary Wiederrecht,|| and Michael R. Wasielewski*,#

Department of Physical Chemistry, University of Freiburg, Albertstr. 21, D-79104 Freiburg, Germany, Department of Physical Chemistry and The Farkas Center for Light-Induced Processes, The Hebrew University of Jerusalem, Jerusalem 91904, Israel, Argonne National Laboratory, Argonne, Illinois 60439-4831, and Department of Chemistry, Northwestern University, Evanston, Illinois 60208-3113

Received: May 10, 2001; In Final Form: August 29, 2001

Using high time resolution Q-band EPR we have been able to identify three different radical pairs generated by pulsed laser excitation of the fixed distance triad consisting of a zinc-9-desoxo-meso-methylpyrochlorophyllide donor (ZC), a pyromellitimide primary acceptor (PI), and a naphthalene-1,8:4,5-diimide secondary acceptor (NI), i.e., ZC−PI−NI, *oriented* in a liquid crystal. Analysis of the transient EPR spectra provides direct evidence for sequential electron transfer from the primary to the secondary radical pair of the triplet channel. At room temperature, this process occurs with an exponential time constant of $\tau_{T,2} = 50 \pm 1$ ns. In the singlet-initiated channel, the intramolecular electron-transfer rates are too fast for direct EPR detection. Thus, even the secondary singlet radical pair $[ZC^{\bullet+}PINI^{\bullet-}]_S$ is formed instantaneously on the time scale of the EPR experiment. The species decays with a time constant of $\tau_{S,3} = 36 \pm 1$ ns by charge recombination to the singlet ground state. The time evolution of the transverse magnetization exhibits fast initial oscillations, which disappear 50 ns after the laser pulse. Model calculations indicate that these oscillations can be assigned to *zero quantum electron precessions* in $[ZC^{\bullet+}PINI^{\bullet-}]_S$. Thus, for the first time, *quantum beats* have been observed from a spin-correlated radical pair, oriented in a liquid crystal.

I. Introduction

It is well established that the light-induced charge separation and the sequential electron transfer in the photosynthetic apparatus proceed via spin-correlated radical pairs as short-lived intermediates.[1−3] In natural photosynthesis, these correlated radical pairs are created in a singlet state, determined by the spin multiplicity of the primary donor, i.e., the "special pair".[4] Generally, such a singlet radical pair is formed with spin-correlated populations of only one-half of the eigenstates, which gives rise to high electron spin polarization.[2,3] Moreover, there are coherences between the eigenstates of the correlated radical pair, which can manifest themselves as *quantum beats* in a time-resolved EPR experiment with adequate time resolution.[5−12]

Attempts to mimic natural photosynthesis by molecular design and architecture of model systems have not been fully accomplished yet. In all cases that were studied, both the singlet and triplet were found to initiate in parallel the intramolecular electron transfer to produce the correlated radical pairs. The scheme in Figure 1a depicts the various processes involved.

A characteristic feature, typical of long-range intramolecular electron transfer, i.e., >12 Å distance, is the occurrence of coherence effects, which lead to fast initial oscillations in the transverse magnetization of the correlated radical pair.[5−12] So far, these quantum beats have been observed in photosynthetic reaction centers[7,9−11] and in a model system[12] under slow-motional conditions, where anisotropic magnetic interactions dominate.

As was demonstrated in previous studies, liquid crystals are powerful solvents not only in accommodating donor−spacer−acceptor systems but also in maintaining the fluid and order properties over a wide range of temperatures. Moreover, because the liquid crystals attenuate the intramolecular electron-transfer rates substantially, it is evident that by employing time-resolved EPR details associated with the intramolecular electron transfer can be observed and extracted from the EPR spectra.[13]

We report here on the first observation of quantum beats from a correlated radical pair in a photosynthetic model, *oriented* in a liquid crystal, i.e., the nematic phase of E-7.[13] The triad, ZC−PI−NI, consists of a chlorophyll-like electron donor, zinc chlorin (ZC), covalently linked to two electron acceptors with different reduction potentials, i.e., pyromellitimide (PI) and 1,8:4,5-naphthalenediimide (NI) (Figure 1b).[14] Although this molecular system was extensively studied by time-resolved EPR, the important features, namely, the detailed genesis of the correlated radical pairs and the associated coherence phenomena, escaped detection because of relatively low time resolution.

II. Experiments and Methods

Sample preparation was discussed in detail in a recent publication.[14] The time-resolved EPR measurements were performed by using a newly developed transient Q-band (35 GHz) bridge (Bruker ER 050 QGT) in combination with a Bruker ESP 300E console. The sample ($\sim 5 \times 10^{-4}$ M) was irradiated in a cylindrical cavity with a loaded Q of ap-

† Part of the special issue "Noboru Mataga Festschrift".

* To whom correspondence should be addressed. E-mail: kothe@pc1.chemie.uni-freiburg.de. Fax: 0049-761-203 6222.

‡ University of Freiburg.

§ The Hebrew University of Jerusalem.

|| Argonne National Laboratory.

Northwestern University.

10.1021/jp011805b CCC: $22.00
Published on Web 10/11/2001

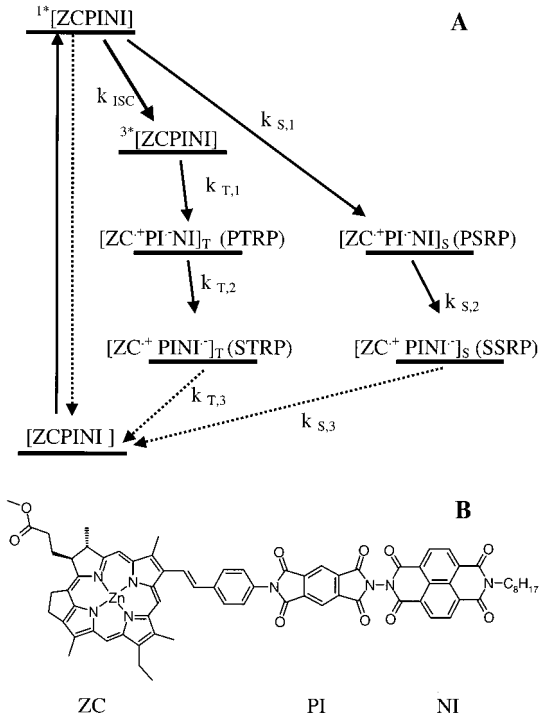

Figure 1. (a) Photoexcited and radical pair states of the triad and relevant interconversion pathways. The energies of the various states have been estimated from EPR spectroscopic data in liquid crystals and from electrochemical data in polar isotropic solvents.[14] (b) Molecular structure of the triad, ZC−PI−NI, indicating the chlorophyll-like donor, ZC, and the two electron acceptors, PI and NI.

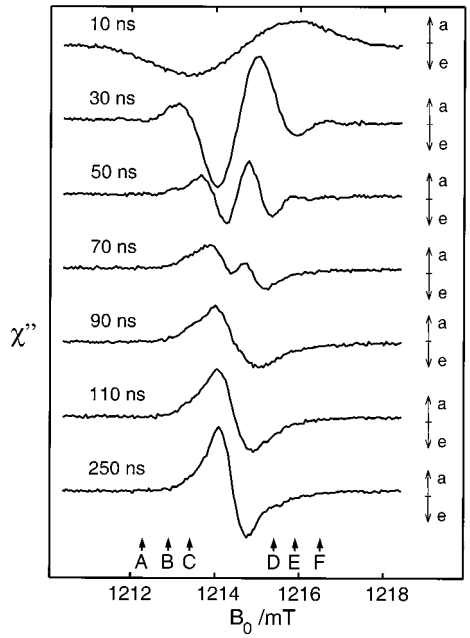

Figure 2. Transient Q-band EPR line shapes of light-induced radical pairs in the partially oriented triad, ZC−PI−NI, at various times after the laser pulse. Positive and negative signals indicate absorptive and emissive polarizations, respectively. Microwave field, $B_1 = 0.061$ mT. Microwave frequency, $\omega/2\pi = 34.0450$ GHz, $T = 295$ K. The solvent is the nematic phase of E-7.[13] Various field positions are marked from A to F. The time evolution of the transverse magnetization at those field positions is shown in Figure 5.

proximately 700, which corresponds to a bandwidth of 50 MHz. The time resolution of the experimental setup is in the 10 ns range. A frequency counter (HP 5352 B) was used to monitor the microwave frequency. The magnetic field was calibrated against Li:LiF (Institute of Crystallography, Moscow), which is a good standard for low-temperature measurements.[15] Optical excitation was carried out with an OPO system (OPTA GmbH), pumped by a Nd:YAG laser (Spectra Physics Quanta Ray GCR 190−10) at a wavelength of 640 nm and with a pulse width of 2.5 ns. For the actual experiment, the intensity was attenuated to approximately 3 mJ/pulse. To avoid photoselection, the laser beam was passed through a quartz depolarizer. The repetition rate of the laser was 10 Hz. A transient recorder (LeCroy 9354A) with a digitizing rate of 2 ns/11 bit sample was used to acquire the time dependent EPR signal. To eliminate the laser background signal, 1500 transients were accumulated at off-resonance conditions and subtracted from those on-resonance. A weak zinc chlorin triplet signal, superimposed on the radical pair signal, was subtracted by using a linear interpolation procedure.

III. Results and Discussion

We show in Figure 1a the photoexcited and radical pair states of the triad and the relevant interconversion pathways. The energies of these states have been estimated from EPR spectroscopic data in liquid crystals and from electrochemical data in polar isotropic solvents.[14] Notably, there are two different routes of producing the secondary radical pairs, $[ZC^{\bullet+}PINI^{\bullet-}]_S$ and $[ZC^{\bullet+}PINI^{\bullet-}]_T$, namely, the singlet and the triplet intramolecular electron-transfer path. In both routes, we have included the primary radical pairs, $[ZC^{\bullet+}PI^{\bullet-}NI]_S$ and $[ZC^{\bullet+}PI^{\bullet-}NI]_T$, which in principle might be observable by high time resolution EPR due to the increased lifetime in a liquid crystalline matrix.[13]

The objective of this study is the characterization of the various radical pair intermediates in the photoexcited triad. To achieve this goal, a solution of the triad in the nematic phase of E-7 was irradiated with short laser pulses and the time evolution of the transverse magnetization was monitored at various static magnetic fields. Generally, a complete EPR data set consists of transient signals taken at equidistant field points covering the total spectral width. This yields a two-dimensional variation of the signal intensity with respect to both the magnetic field and the time axis. Transient spectra can be extracted from this plot at any time after the laser pulse as slices parallel to the magnetic field axis. Likewise, the time evolution of the transverse magnetization may be obtained for any given field as a slice along the time axis. In the following, transient spectra and time profiles are discussed separately.

Typical EPR line shapes, observed 10, 30, 50, 70, 90, 110, and 250 ns after the laser pulse, are shown in Figure 2. The spectra refer to a microwave frequency of $\omega/2\pi = 34.0450$ GHz (Q-band), a microwave field of $B_1 = 0.061$ mT and $T = 295$ K. Note that a positive signal indicates absorptive (a) and a negative emissive (e) spin polarization. Evidently, the very early spectra (10 and 30 ns) are much broader than the later ones, which we attribute to lifetime broadening. Moreover, the spectral shape changes drastically with time, indicating at least three different short-lived radical pairs. The central part of the 50 ns spectrum with an e/a polarization pattern is attributed to the secondary radical pair, $[ZC^{\bullet+}PINI^{\bullet-}]_S$, of the singlet route. Support for this assignment comes from time-resolved EPR spectra taken with photoexcitation at 535 nm, which predominantly display photoproducts from the singlet channel (results not shown).

Closer inspection of the wings of the 50 ns line shape indicates an additional spectrum of ∼1.6 mT width exhibiting an a/e polarization pattern. The characteristics of this spectrum,

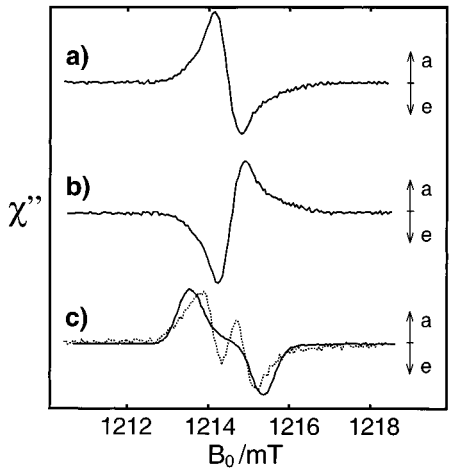

Figure 3. Transient Q-band EPR spectra of various light-induced radical pairs formed during sequential electron transfer in the partially oriented triad, ZC−PI−NI. Positive and negative signals indicate absorptive and emissive polarizations, respectively. Other experimental parameters are as in Figure 2. (a) EPR spectrum of the secondary radical pair, $[ZC^{\bullet+}PINI^{\bullet-}]_T$, in the triplet channel. (b) EPR spectrum of the secondary radical pair, $[ZC^{\bullet+}PINI^{\bullet-}]_S$, in the singlet channel. (c) Full line: EPR spectrum observed for the photoexcited diad, ZC−PI. Dashed line: EPR spectrum of the primary radical pair, $[ZC^{\bullet+}PI^{\bullet-}NI]_T$, in the triplet channel.

most clearly visible 70 ns after the laser pulse, are consistent with those observed for the photoexcited diad, ZC−PI, suggesting an assignment to the primary radical pair, $[ZC^{\bullet+}PI^{\bullet-}NI]_T$, of the triplet route. Note, however, that the 70 ns EPR spectrum further evolves in time, resulting in a narrow a/e spectrum of 1 mT width at 250 ns, which we assign to the secondary radical pair, $[ZC^{\bullet+}PINI^{\bullet-}]_T$, of the triplet channel.

Thus, except for the late EPR spectrum at 250 ns, all other spectra are admixtures of three different radical pairs, i.e., they contain spectral contributions from the primary triplet radical pair $[ZC^{\bullet+}PI^{\bullet-}NI]_T$, secondary triplet radical pair $[ZC^{\bullet+}PINI^{\bullet-}]_T$, and secondary singlet radical pair $[ZC^{\bullet+}PINI^{\bullet+}]_S$. Because the EPR spectra of the latter two radical pairs result from the same species but different precursors, they should differ from each other only by exhibiting opposite phases.[14] Therefore, one can invert the experimental 250 ns EPR spectrum (Figure 3a) and safely assign it to the spectrum of the corresponding singlet radical pair (Figure 3b). As will be discussed below, the two radical pair spectra cancel each other at a particular point in time, thus, leaving only the EPR spectrum which we attribute to the primary radical pair of the triplet channel. Indeed, the polarization and width of this spectrum fits fairly well with the spectrum of the photoexcited diad, ZC−PI,[14] depicted in Figure 3c (solid line).

The above analysis suggests that the observed EPR line shape, $f(B_0,t)$, can be described as a time-dependent superposition of three radical pair spectra denoted by $f_{PTRP}(B_0)$, $f_{STRP}(B_0)$, and $f_{SSRP}(B_0)$. Here the indices indicate the primary triplet radical pair, the secondary triplet radical pair, and the secondary singlet radical pair, respectively. Using the kinetic scheme, introduced in Figure 1a, the following model function is derived:

$$f(B_0,t) = A_{PTRP}(t)\, f_{PTRP}(B_0) + A_{STRP}(t)\, f_{STRP}(B_0) + A_{SSRP}(t)\, f_{SSRP}(B_0) = [A_{STRP}(t) - A_{SSRP}(t)]\, f_{STRP}(B_0) + A_{PTRP}(t)\, f_{PTRP}(B_0) \quad (1)$$

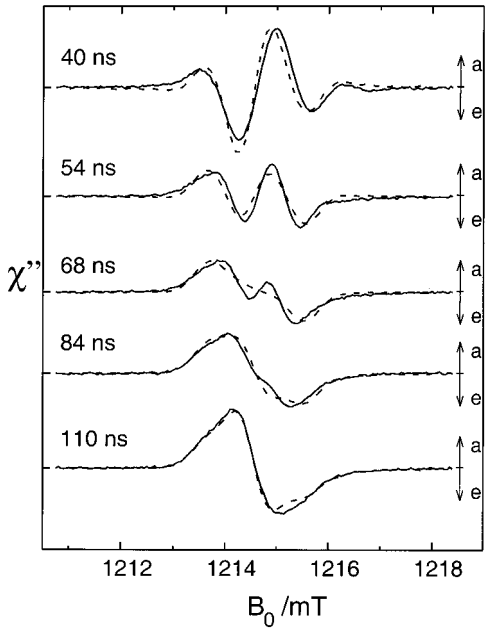

Figure 4. Transient Q-band EPR line shapes of light-induced radical pairs in the partially oriented triad, ZC−PI−NI, at various times after the laser pulse. Positive and negative signals indicate absorptive and emissive polarizations, respectively. Other experimental parameters are as in Figure 2. Full lines: experimental line shapes. Dashed lines: calculated line shapes, using the kinetic model for the formation and decay of the radical pairs, i.e., $[ZC^{\bullet+}PI^{\bullet-}NI]_T$, $[ZC^{\bullet+}PINI^{\bullet-}]_T$, and $[ZC^{\bullet+}PINI^{\bullet-}]_S$. The kinetic parameters are listed in Table 1.

where the time dependence of the spectral amplitudes is given by

$$A_{PTRP}(t) = A_{PTRP}(0)\exp(-t/\tau_{T,2}) \quad (2)$$

$$A_{STRP}(t) = A_{PTRP}(0)\frac{1/\tau_{T,2}}{1/\tau_{T,3} - 1/\tau_{T,2}}[\exp(-t/\tau_{T,2}) - \exp(-t/\tau_{T,3})] \quad (3)$$

$$A_{SSRP}(t) = A_{SSRP}(0)\exp(-t/\tau_{S,3}) \quad (4)$$

Here $\tau_{T,2} = 1/k_{T,2}$ and $\tau_{S,3} = 1/k_{S,3}$ are exponential time constants associated with the formation and the decay of particular radical pairs and $\tau_{T,3}$ is an electron spin relaxation time. Values for $\tau_{T,2}$, $\tau_{S,3}$, and $\tau_{T,3}$ have been obtained by fitting the model function to the experimental EPR line shapes observed in the time range from 40 to 250 ns. The result of such a computer fit, in which $f_{PTRP}(B_0)$ was approximated by the spectrum of the photoexcited diad, is shown in Figure 4. Generally, the calculated EPR line shapes (dashed lines) compare favorably with their experimental counterparts (solid lines). Thus, we conclude that the kinetic model used in the analysis is basically correct.

Table 1 summarizes the parameter values obtained from the fit. In the triplet initiated route, intramolecular electron transfer between the primary and secondary radical pair occurs with a time constant of 50 ± 1 ns. Evidently, high time resolution is required to characterize this process. To our knowledge, such a short electron transfer time has not previously been determined by EPR. Monitoring this fast intramolecular electron transfer process enabled us to assign the late experimental EPR spectrum exclusively to $[ZC^{\bullet+}PINI^{\bullet-}]_T$. As to the identification of the primary radical pair, formed in the triplet channel, the assign-

TABLE 1: Kinetic Parameters Obtained from the Analysis of Transient Q-Band EPR Spectra of Light-Induced Singlet and Triplet Radical Pairs in the Partially Oriented Triad[a]

time constants[a]		assignment
$\tau_{T,2}$	50 ± 1 ns	Electron transfer between triplet radical pairs[b]
$\tau_{T,3}$	1.1 ± 0.1 μs	Relaxation time of secondary triplet radical pair
$\tau_{S,3}$	36 ± 1 ns	Charge recombination of secondary singlet radical pair[c]

[a] The underlying kinetic model is shown in Figure 1a. [b] Intramolecular electron transfer between primary and secondary triplet radical pair. [c] Charge recombination to the singlet ground state.

ment can be tested using the kinetic model. Inspection of eq 1 reveals that the EPR spectrum of $[ZC^{\bullet+}PINI^{\bullet-}]_T$ vanishes completely at a particular point in time. Here the spectral contributions of both secondary radical pairs cancel each other, thus, leaving only the EPR spectrum of the primary radical pair, $[ZC^{\bullet+}PI^{\bullet-}NI]_T$, of the triplet channel. Evaluating this point in time on the basis of the parameters of Table 1 yields $t = 67$ ns. The superimposed dashed line in Figure 3c corresponds to the EPR spectrum deduced for $[ZC^{\bullet+}PI^{\bullet-}NI]_T$, which is roughly close to that of the photoexcited diad, ZC−PI (solid line). The apparent discrepancy between the two spectra is probably due to the different spin distribution in $[ZC^{\bullet+}PI^{\bullet-}NI]$ and $[ZC^{\bullet+}PI^{\bullet-}]$.

In the singlet-initiated channel (Figure 1a), the intramolecular electron transfer rates are too fast for direct EPR detection, even in the liquid crystalline environment. Indeed, the very early spectra exhibit lifetime broadening implying that the secondary radical pair, $[ZC^{\bullet+}PINI^{\bullet-}]_S$, is formed instantaneously on the time scale of the EPR experiment. This is in agreement with optical data suggesting extremely fast intramolecular electron transfer in the singlet channel.[16] It is evident that even in the liquid crystalline environment the formation rate of $[ZC^{\bullet+}PINI^{\bullet-}]_S$ escapes EPR detection. Only a decay time of 36 ± 1 ns could be determined (Table 1). We assign this time constant to fast charge recombination to the singlet ground state (Figure 1a).

Let us now discuss the time evolution of the transverse magnetization, measured at six selected field positions taken symmetrically about the center position (Figure 5, left column). The transients refer to a microwave frequency of $\omega/2\pi = 34.0450$ GHz, a microwave field of $B_1 = 0.061$ mT, and $T = 295$ K. Evidently, there are fast initial oscillations which disappear 50 ns after the laser pulse. Notice that these oscillations are most conspicuous at the two edges of the spectrum, corresponding to positions A and F. Fourier transformation of the time profiles yields oscillation frequencies from 30 to 50 MHz. In view of previous studies,[7,9−12] we assign these oscillations to quantum beats associated with the nonadiabatic generation of the secondary radical pair, $[ZC^{\bullet+}PINI^{\bullet-}]_S$, of the singlet channel.

If one assumes that the rotational correlation time, τ_c, of the triad is slow, i.e., $\tau_c\Delta\omega_{RP} > 1$, where $\Delta\omega_{RP}$ denotes the anisotropy of the magnetic interactions in the radical pair, it is possible to analyze the EPR transients using a slow-motional model.[6,9,11] Generally, a photoinduced correlated radical pair is created with spin-correlated populations of only one-half of the eigenstates and with *zero quantum electron coherence* between these states.[2,3,5−12] In the absence of a microwave field, the eigenstate populations are constant in time, whereas the zero quantum electron coherences[5−12] oscillate at distinct frequencies, given by the energy separation of the corresponding eigenstates.[8,11] The continuous microwave field, applied in transient EPR, has two effects. First, it converts the longitudinal magnetization associated with the population differences between neighboring eigenstates into transverse magnetization. This gives the Torrey oscillations.[17] Second, it converts the zero quantum electron coherences into observable single quantum precessions or quantum beats, observable in EPR experiments with adequate time resolution.[7,9−12]

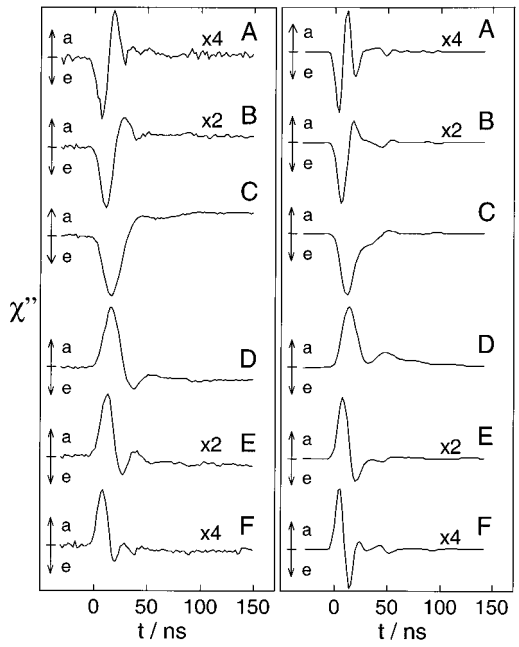

Figure 5. Time evolution of the transverse magnetization of the light-induced singlet radical pair, $[ZC^{\bullet+}PINI^{\bullet-}]_S$, in the partially oriented triad, ZC−PI−NI, immediately after the laser pulse. The transients refer to six different static magnetic fields (positions A−F, Figure 2). Positive signals indicate absorptive and negative emissive polarizations, respectively. Other experimental parameters are as in Figure 2. Left column: experimental time profiles. Right column: calculated time profiles, using the parameters given in Table 2.

Under slow-motional conditions, the frequency of the *zero quantum electron precessions*, ω_{ZQ}, critically depends on the orientation, $\Omega \equiv (\Phi, \Theta, \Psi)$, of the radical pair in the laboratory frame, **x**, **y**, **z**. As shown previously,[9,10,12] ω_{ZQ} is given by

$$\omega_{ZQ} = (1/\hbar)\left\{\left[\frac{2}{3}D^{zz}(\Omega) - 2J_{ex}\right]^2 + [(g_1^{zz}(\Omega) - g_2^{zz}(\Omega))\mu_B B_0 + \sum_k A_{1k}^{zz}(\Omega)M_{1k}^i - \sum_l A_{2l}^{zz}(\Omega)M_{2l}^j]^2\right\}^{1/2} \quad (5)$$

$$M_{1k}^i = I_{1k}, I_{1k} - 1, ..., -I_{1k} \quad (6)$$

$$M_{2l}^j = I_{2l}, I_{2l} - 1, ..., -I_{2l} \quad (7)$$

where $D^{zz}(\Omega)$, J_{ex}, $g_i^{zz}(\Omega)$, μ_B, B_0, and $A_{ij}^{zz}(\Omega)$ are the *zz* component of the dipolar coupling tensor, the strength of the isotropic exchange interaction, the *zz* component of the *g* tensor of radical *i*, the Bohr magneton, the static magnetic field, and the secular part of the hyperfine interaction between nucleus *j* and radical *i*, respectively. The weak B_1 field, commonly employed in transient EPR, allows for only a small range of orientations to meet the resonance condition. Consequently, we expect the frequencies of the zero quantum electron precessions to vary significantly with B_0 across the EPR spectrum, as observed experimentally (Figure 5, left column).

TABLE 2: Parameters Used in EPR Model Calculations for the Light-Induced Singlet Radical Pair, $ZC^{\bullet+}PINI^{\bullet-}$, in the Partially Oriented Triad

	g factor[a]	a_N (mT)[b]	a_H (mT)[b]
$ZC^{\bullet+}$	2.0027	0.29 (2×)	0.21 (3×)
$NI^{\bullet-}$	2.0031	0.10 (2×)	0.19 (4×)
dipolar coupling,[c] *D* (mT)	−0.48		
spin−spin coupling,[c] *J* (mT)	0.20		
microwave frequency, $\omega/2\pi$ (GHz)	34.0450		
microwave field, B_1 (mT)	0.061		
decay time,[d] $\tau_{S,3}$ (ns)	36		
inhomog. broadening, ΔB_0 (mT)	0.15		
orientational order,[e] *A*	4.5		
order parameter,[e] S_{ZZ}	0.6		

[a] Estimated values on the basis of published data.[19,12] [b] Adapted from X-band EPR studies of related radical ions.[19,20] [c] The spin−spin coupling parameters are estimates based on the molecular structure of the triad.[12,14] [d] The lifetime of the radical pair was determined in the present study (see Table 1). [e] Estimated values for the triad in E-7.

The anisotropic distribution of the radical pairs in a liquid crystalline medium can be considered by the orientational distribution function[18]

$$f(\beta) = N \exp(A \cos^2 \beta) \tag{8}$$

$$\cos \beta = \cos \Theta \cos \xi - \sin \Theta \cos \Psi \sin \xi \tag{9}$$

Here, *N* is a normalization constant and β is the angle between the symmetry axis, **Z**, of the order tensor and the director axis (net ordering axis), **z′**. The coefficient *A* in eq 8 characterizes the alignment of the radical pairs along the director axis, whereas the angle ξ specifies the orientation of **z′** in the laboratory frame. In nematic liquid crystals with a positive diamagnetic anisotropy, the director orients parallel to the magnetic field, i.e., $\xi = 0°$. The orientational order parameter, S_{ZZ}, is related to the coefficient *A* by a mean value integral

$$S_{ZZ} = \frac{1}{2} N \int_0^{\pi} (3 \cos^2 \beta - 1) \exp(A \cos^2 \beta) \sin \beta \, d\beta \tag{10}$$

To establish the observation of quantum beats, model calculations have been performed for the secondary radical pair of the singlet channel. Table 2 summarizes the parameters used in the calculations. Approximate values for the *g* factors of $ZC^{\bullet+}$ and $NI^{\bullet-}$ could be obtained on the basis of published data.[19,12] The spin−spin coupling parameters are estimates based on the molecular structure of the triad (Figure 1).[12,14] Hyperfine interactions were considered by using published nitrogen and proton hyperfine couplings for related radical ions.[19,20] The decay time of $[ZC^{\bullet+}PINI^{\bullet-}]_S$ was determined in the present study (Table 1). Inhomogeneous broadening was considered by convolution with a Gaussian of line width $\Delta B_0 = 0.15$ mT.

In Figure 5, we compare experimental (left column) and calculated time profiles (right column) at early times after light excitation. In the calculations, the order and dipolar tensor were assumed to be collinear. In addition, the limited bandwidth of the cavity was considered by using a band-pass filter at 50 MHz. Generally, the calculated time profiles compare reasonably with their experimental counterparts. In particular, the phase and frequency of the fast initial oscillations and their dependence on the static magnetic field is satisfactorily reproduced by the calculations. Evidently, the assignment of these oscillations to zero quantum electron precessions in $[ZC^{\bullet+}PINI^{\bullet-}]_S$ is correct. Thus, for the first time, quantum beats have been observed from a correlated radical pair, oriented in a liquid crystal. Further studies along these lines are currently in progress.

IV. Conclusions

Light-induced quantum beat oscillations have been observed for a correlated radical pair, oriented in a liquid crystal. Compared to previous studies of this phenomenon, the use of macroscopically aligned samples provides more precise information on the spin dynamics of the short-lived intermediates of photosynthesis. Therefore, a thorough study of these coherences in well-aligned liquid crystals appears promising for the elucidation of the mechanism of the primary events of photosynthesis.

Acknowledgment. Financial support by the Deutsche Forschungsgemeinschaft (Ko/16-3; Schwerpunktprogramm Hochfeld-EPR) is gratefully acknowledged. This work is in partial fulfillment of the requirements for a Ph.D. degree (E.S.) at the Hebrew University of Jerusalem. This work was partially supported by the US−Israel BSF and the Volkswagen Foundation. The Farkas Center is supported by the Bundesministerium für Forschung und Technologie and the Minerva Gesellschaft für Forschung GmbH, FRG. Work at Northwestern was supported by the Division of Chemical Sciences, Office of Basic Energy Sciences, U. S. Department of Energy under Grant No. DE-FG02-99ER14999.

References and Notes

(1) Thurnauer, M. C.; Norris, J. R. *Chem. Phys. Lett.* **1980**, *76*, 557.
(2) Closs, G. L.; Forbes, M. D. E.; Norris, J. R. *J. Phys. Chem.* **1987**, *91*, 3592.
(3) Buckley, C. D.; Hunter, D. A.; Hore, P. J.; McLauchlan, K. A. *Chem. Phys. Lett.* **1987**, *135*, 307.
(4) Norris, J. R.; Uphaus, R. A.; Crespi, H. L.; Katz, J. J. *Proc. Natl. Acad. Sci. U.S.A.* **1971**, *68*, 625.
(5) Salikhov, K. M.; Bock, L. H.; Stehlik, D. *Appl. Magn. Reson.* **1990**, *1*, 195.
(6) Bittl, R.; Kothe, G. *Chem. Phys. Lett.* **1991**, *177*, 547.
(7) Kothe, G.; Weber, S.; Bittl, R.; Ohmes, E.; Thurnauer, M. C.; Norris, J. R. *Chem. Phys. Lett.* **1991**, *186*, 474.
(8) Zwanenburg, G.; Hore, P. J. *Chem. Phys. Lett.* **1993**, *203*, 65.
(9) Kothe, G.; Weber, S.; Ohmes, E.; Thurnauer, M. C.; Norris, J. R. *J. Phys. Chem.* **1994**, *98*, 2706.
(10) Kothe, G.; Weber, S.; Ohmes, E.; Thurnauer, M. C.; Norris, J. R. *J. Am. Chem. Soc.* **1994**, *116*, 7729.
(11) Kothe, G.; Bechtold, M.; Link, G.; Ohmes, E.; Weidner, J. U. *Chem. Phys. Lett.* **1998**, *283*, 51.
(12) Kiefer, A. M.; Kast, S. M.; Wasielewski, M. R.; Laukenmann, K.; Kothe, G. *J. Am. Chem. Soc.* **1999**, *121*, 188.
(13) Levanon, H.; Hasharoni, K. *Prog. React. Kinet.* **1995**, *20*, 309.
(14) Levanon, H.; Galili, T.; Regev, A.; Wiederrecht, G. P.; Svec, W.; Wasielewski, M. R. *J. Am. Chem. Soc.* **1998**, *120*, 6366.
(15) Cherkasov, F. G.; Denisenko, G. A.; Vitols, A. Y.; L'vov, S. G. In *Proceedings of the XXVII th Congress Ampere on Magnetic Resonance and Related Phenomena*; Salikhov, K. M., Ed.; Zavoisky Physical-Technical Institute: Kazan, Russia, 1994; Vol. 1, pp 416−417.
(16) Wiederrecht, G. P.; Niemczyk, M. P.; Svec, W. A.; Wasielewski, M. R. *J. Am. Chem. Soc.* **1996**, *118*, 81.
(17) Torrey, H. *Phys. Rev.* **1949**, *76*, 1059.
(18) Berthold, T.; Bechtold, M.; Heinen, U.; Link, G.; Poluektov, O.; Utschig, L.; Tang, J.; Thurnauer, M. C.; Kothe, G. *J. Phys. Chem. B* **1999**, *103*, 10733.
(19) Fajer, J.; Borg, D. C.; Forman, A.; Dolphin, D.; Felton, R. H. *J. Am. Chem. Soc.* **1973**, *95*, 2739.
(20) Nelsen, S. F. *J. Am. Chem. Soc.* **1967**, *89*, 5925.